Supplementary Information to:

Late-stage evolution of the Crotone Mud Volcano and implications for mud volcanism in the Calabrian Accretionary Prism

Lisi, G.[1,2*], Pellegrini, C.[1], Argentino, C.[3], Insinga, D.[4], Capotondi, L.[1], Panieri, G.[3,5], Tassi, F.[6], Rovere, M.[1]

[1] Institute of Marine Sciences, Consiglio Nazionale delle Ricerche (CNR-ISMAR), Bologna, Italy

[2] Department of Biological, Geological, and Environmental Sciences, Alma Mater Studiorum, University of Bologna, Italy

[3] Department of Geosciences, the Arctic University of Norway (UiT), Tromsø, Norway

[4] Institute of Marine Sciences, Consiglio Nazionale delle Ricerche (CNR-ISMAR), Napoli, Italy

[5] Istituto di Scienze Polari, Consiglio Nazionale delle Ricerche (CNR-ISP), Bologna, Italy

[6] Dipartimento di Scienze della Terra, University of Florence, Italy

*Corresponding Author: Giulia Lisi giulialisi@cnr.it

Cruise name	Sediment core	Latitude [N]	Longitude [E]	Water depth [m]	Core length [m]	Sector
Pioneer	GC08	39° 4' 13.1"	17° 21' 34"	607	1.78	Central
Pioneer	GC09	39° 3' 55.7"	17° 21' 27.1"	612	3.29	Northern-central
Ecorest Pioneer	GC01	39° 4' 19.8"	17° 21' 21.6"	612	3.09	Southern
Pioneer	PC12	39° 3' 41"	17° 21' 23.6"	590	8.52	Outside CMV (reference core)

Supplementary Table S1: Information for the sediment cores collected within different sectors of the Crotone Mud Volcano (GC08, GC09, GC01) and at the reference site (PC12).

Core - sample code	Material	Stratigraphic relation to tephra	^{14}C Age (B.P.)	^{14}C Calibrated Age (B.P.) - median	^{14}C Calibrated Age (B.P.) range (2σ)	δ^{13}C (‰)
PC12 50u	*U. peregrina*	1 cm below t1	2640 ± 61	2420	2136 - 2704	-7.3
PC12 525-526	*U. peregrina*	30 cm above t4	13433 ± 97	15476	15216 - 15996	-14.5
PC12 760-761	*U. peregrina*	/	19507 ± 124	22701	22406 - 23163	-13.3

Supplementary Table S2: Radiocarbon ages of *U. peregrina* specimens analyzed from reference core PC12. Stratigraphic relationships with tephra layers are also reported.

Tephrostratigraphy

The complete analytical dataset of t1 to t4 tephra layers can be found in Tables S1-S5. whereas the average single glass composition is reported in Table S6.

Tephra t1

This layer occurs from 51 cm to 46 cm bsf in PC12. It is normally graded and characterized by light and light grey micropumice, which pass upwards to microscoria and leucite bearing lithics. Loose crystals of feldspar, plagioclase, and biotite occur throughout the deposit. To better characterize these thick deposits, two subsamples were selected, PC12/IX-47.5 and PC12/IX-49. The analyzed glasses are phonolites with few points straddling the boundary with the tephriphonolite field (Fig. 4a). Tephra t1 can be correlated also in core GC09 (Fig. 3). It is a fine ash made up equally of light and light grey micropumice, microscoria, lithics and loose crystals of feldspar, plagioclase and large amounts of biotite. This ~ 8 cm thick deposit is mixed with a coarse clastic sediment characterized by rounded and sub-rounded grey, light and dark grey components. Sample GC09/III-133.5 representative of tephra t1 displays a chemical composition which completely overlaps that of PC12 samples (Fig. 4a, b). XRF-derived proxies show diagnostic peaks within the tephra t1 interval in both PC12 and the southern sector in ln(Zr/Rb), ln(Ba/Ti), ln(Sr/Ti) and ln(Nb/Ti), further supporting their correlation (Fig. 3). The same geochemical signature is also observed in the northern-central sector (Figs. 2, 3). Lithology (e.g. the occurrence of leucite), (geo)chemical features and the stratigraphic position, suggest a correlation of tephra t1 with products erupted by Somma-Vesuvius at 79 CE during the explosive event, which destroyed the cities of Pompeii and Ercolano[1]. It produced the tephra marker Z-1, widely dispersed in the central Mediterranean. In detail, as also reported for other sites close to the study area, the composition of both white and grey pumice, which typically characterize the fall sequence on land, is found in tephra t1[2-5] (Fig. 4b).

Cryptotephra t2

This cryptotephra, marked by a pronounced magnetic susceptibility peak along the record, is a very fine ash formed by dark scoriae, lithics, loose crystal of feldspar, pyroxene, olivine and mica, which are mixed with the bioclastic portion. The rare interstitial glass within the microlite groundmass in the juvenile materials hampered its chemical characterization. On the contrary, the composition of clinopyroxene helps to link cryptotephra t2 with Mt. Etna activity (Fig. 4c).

According to the stratigraphic position (below tephra t1/79 CE) and similar occurrences in the Taranto Bay[6-8] and in the Ionian Sea[3,9] cryptotephra t2 might be correlated with the scoria fall events of FL (3361 ± 76 cal years BP) or FS (4360 ± 92 cal years BP)[10]. FL event, in particular, produced a good stratigraphic marker spread towards the eastern sector of the volcano up to the Balkans (e.g. [11]).

Cryptotephra t3

Cryptotephra t3 is a very fine ash characterized by transparent glass shards with elongated and thin bubble wall morphologies. The volcanic portion approximates the 100% of the total volume of the analyzed sample (PC12/VI-261). The composition is rhyolitic (Fig. 4a) with High-K Calc-alkaline affinity which is typical of Aeolian Islands activity (Fig. 4d). Chemical features along with the stratigraphic position within the S1 sapropelic facies, suggest a correlation of cryptotephra t3 with the Vallone del Gabellotto proximal products from Lipari[12]. The corresponding marine tephra marker (E-1)[13] was dated in the marine realm at ca 8.43 cal ka - 8.73 cal ka[14,15] and found from the southern Tyrrhenian Sea up to Greece[16].

Tephra t4

This deposit occurs at 563 cm bsf. It is a fine - grained black ash made up of minor dark grey micropumices with spherical vesicles, dark scoriae and loose crystals of clinopyroxene and plagioclase. It represents the 50% of the total sediment. Glasses have a Na- alkaline affinity and a trachytic composition (qz-norm) with few points close to the benmoreite field (Fig. 4a). These chemical features are consistent with a correlation of t4 with Mt. Etna deposits. The calibrated radiocarbon age of 15.476 ± 97 years obtained at 525 cm - 526 cm bsf locates tephra t4 in the late glacial explosive activity of the volcano, which was chemically and chronologically constrained by Albert et al.[17] based on terrestrial and marine archives. In detail, tephra t4 represents the occurrence in the study area of the Y-1 marker tephra[2] sourced by the Biancavilla-Montalto Ignimbrite event (Unit D[10]) and found with such chemical features in the Ionian Sea. in the southern Adriatic Sea and Libya (Fig. 4e). The Biancavilla-Montalto Ignimbrite/Y-1 was radiocarbon dated at ca. 17 cal ka BP[18]. The astronomical tuning of core KC01B in the Ionian Sea gives a slightly younger result of 16.7 ka for this tephra[19,20]. Anyway, it closes a phase of close in time eruptive events. which started at ca. 19 ka[17].

		SiO_2	TiO_2	Al_2O_3	FeO	MnO	MgO	CaO	Na_2O	K_2O	P_2O_5	Cl	F	S	Original Total
(Tephra) t1 (Z-1)	(Sample) **PC12/IX-47.5**	55.34	0.10	22.97	2.18	0.16	0.22	2.60	7.72	7.58	0.08	0.71	0.26	0.05	98.37
		55.34	0.30	20.85	3.47	0.01	0.45	4.46	6.27	7.41	0.12	0.77	0.49	0.05	96.82
		55.26	0.28	22.70	2.54	0.16	0.14	3.15	7.97	6.32	0.00	0.84	0.61	0.03	99.37
		54.72	0.45	21.16	3.35	0.10	0.55	3.98	5.75	8.49	0.14	0.67	0.46	0.16	98.66
		54.54	0.43	21.20	3.48	0.09	0.52	4.42	5.61	8.58	0.06	0.67	0.21	0.21	98.46
		55.19	0.55	20.81	3.76	0.10	0.59	4.95	6.22	6.43	0.06	0.76	0.47	0.11	98.52
		55.32	0.17	22.90	2.04	0.05	0.13	2.66	7.53	8.05	0.00	0.68	0.44	0.04	98.75
		54.86	0.49	21.10	3.23	0.04	0.42	4.09	5.79	8.68	0.12	0.74	0.30	0.14	98.02
		54.86	0.36	21.22	3.22	0.33	0.39	3.81	5.93	8.40	0.08	0.68	0.58	0.13	98.9
		54.46	0.56	21.26	3.58	0.18	0.44	3.97	5.55	8.56	0.12	0.67	0.47	0.18	99.62
	(Sample) **PC12/IX-49**	56.62	0.27	22.94	2.23	0.10	0.20	4.42	7.70	4.40	0.14	0.69	0.28	0.00	99.04
		54.61	0.58	20.83	4.07	0.06	0.62	4.51	5.44	8.05	0.14	0.69	0.24	0.15	98.60
		55.72	0.14	22.77	2.36	0.04	0.19	2.89	8.05	6.63	0.06	0.75	0.40	0.00	97.11
		55.65	0.21	22.41	2.43	0.22	0.20	2.83	6.51	8.26	0.00	0.66	0.57	0.04	92.00
		55.76	0.30	21.49	2.32	0.12	0.12	3.48	7.33	7.18	0.09	0.98	0.63	0.21	98.28
		54.56	0.26	22.35	2.59	0.15	0.16	2.91	9.31	6.08	0.02	0.87	0.68	0.04	98.34
		55.23	0.53	20.98	3.71	0.09	0.42	3.78	6.27	7.26	0.23	0.80	0.53	0.13	98.29
		55.16	0.22	22.76	2.34	0.17	0.14	3.22	8.57	5.73	0.00	0.86	0.76	0.04	98.32
		55.28	0.18	22.70	2.27	0.10	0.15	2.81	7.79	7.49	0.00	0.75	0.37	0.09	98.31
		55.47	0.28	22.84	2.35	0.05	0.14	2.86	8.37	6.27	0.05	0.71	0.54	0.06	98.39
		55.16	0.53	20.97	3.57	0.08	0.51	4.41	5.76	8.11	0.05	0.72	0.04	0.09	97.76
		55.36	0.42	20.82	3.64	0.17	0.43	4.58	6.46	6.72	0.16	0.73	0.38	0.13	99.06
		54.79	0.50	20.68	3.81	0.14	0.46	4.64	6.34	7.00	0.15	0.81	0.49	0.17	99.14
		55.35	0.24	23.15	2.05	0.20	0.10	2.76	5.72	9.25	0.06	0.76	0.37	0.00	98.62
		54.61	0.15	22.38	2.70	0.10	0.09	3.26	8.13	6.98	0.00	0.92	0.66	0.00	97.76
		55.59	0.06	22.79	2.18	0.10	0.09	2.82	7.76	7.18	0.00	0.74	0.65	0.03	97.95
		54.73	0.48	21.11	3.48	0.26	0.44	4.40	5.85	7.97	0.02	0.74	0.44	0.07	97.57
		55.19	0.15	22.75	2.23	0.20	0.15	3.00	8.16	6.67	0.00	0.76	0.68	0.06	97.02
		54.99	0.46	21.06	3.63	0.02	0.36	4.42	6.52	7.26	0.00	0.72	0.42	0.15	97.88
		54.89	0.51	20.99	3.65	0.08	0.49	4.09	6.19	7.65	0.06	0.79	0.50	0.09	98.57

Supplementary Table S3: SEM-EDS single glass analyses of the Z-1 tephra for PC12 sediment core. All analyses recalculated water-free to 100%. The original totals are reported.

(Tephra) **t1 (Z-1)**	(Sample) **GC09/III-133.5**	**SiO_2**	**TiO_2**	**Al_2O_3**	**FeO**	**MnO**	**MgO**	**CaO**	**Na_2O**	**K_2O**	**P_2O_5**	**Cl**	**F**	**S**	**Original Total**
		56.41	0.37	22.97	2.41	0.08	0.13	2.37	7.28	6.86	0.04	0.71	0.29	0.07	97.28
		54.99	0.32	20.80	3.98	0.08	0.50	4.50	6.68	6.69	0.21	0.83	0.30	0.10	95.95
		55.32	0.00	23.09	2.03	0.08	0.14	2.63	6.92	8.70	0.10	0.70	0.26	0.02	97.65
		54.67	0.51	20.31	4.78	0.23	0.95	4.79	4.27	8.49	0.13	0.62	0.26	0.00	97.02
		54.46	0.54	21.78	2.82	0.00	0.26	3.62	5.26	9.65	0.19	0.68	0.53	0.22	96.73
		54.99	0.32	20.80	3.98	0.08	0.50	4.50	6.68	6.69	0.21	0.83	0.30	0.10	95.95
		55.32	0.00	23.09	2.03	0.08	0.14	2.63	6.92	8.70	0.10	0.70	0.26	0.02	97.65
		54.67	0.51	20.31	4.78	0.23	0.95	4.79	4.27	8.49	0.13	0.62	0.26	0.00	97.02
		54.46	0.54	21.78	2.82	0.00	0.26	3.62	5.26	9.65	0.19	0.68	0.53	0.22	96.73
		55.43	0.32	21.48	3.46	0.16	0.45	3.92	5.56	8.28	0.17	0.58	0.21	0.00	96.62
		54.69	0.28	23.02	2.09	0.14	0.08	2.34	7.15	9.06	0.00	0.68	0.48	0.00	98.05
		50.98	0.79	19.52	6.95	0.09	2.05	7.18	4.45	6.41	0.40	0.83	0.28	0.06	97.45
		55.76	0.41	20.94	3.39	0.19	0.35	3.22	7.16	7.18	0.12	0.76	0.29	0.23	96.4
		55.17	0.39	22.00	2.84	0.19	0.06	3.19	4.87	10.25	0.04	0.74	0.09	0.16	97.5
		55.20	0.52	21.06	3.55	0.19	0.54	3.92	5.73	8.00	0.19	0.64	0.22	0.23	98.39
		55.73	0.54	21.20	3.27	0.21	0.16	2.48	8.06	6.78	0.17	0.89	0.43	0.08	96.69
		55.67	0.45	20.93	3.38	0.15	0.50	4.32	6.65	7.06	0.10	0.73	0.00	0.08	96.52
		55.72	0.51	21.16	3.37	0.12	0.37	3.52	6.51	7.57	0.19	0.75	0.00	0.21	96.18
		55.05	0.43	21.15	3.44	0.00	0.49	3.81	5.90	8.55	0.13	0.68	0.22	0.15	96.4
		55.14	0.51	21.12	3.30	0.25	0.44	3.80	5.85	8.72	0.08	0.68	0.07	0.03	95.71
		55.61	0.29	21.05	3.62	0.04	0.50	4.15	5.99	7.52	0.10	0.81	0.24	0.08	96.22
		55.75	0.61	20.50	3.65	0.18	0.24	3.57	7.12	7.04	0.02	0.85	0.22	0.25	98.07
		56.19	0.32	20.64	3.28	0.13	0.24	3.91	3.84	10.44	0.03	0.63	0.28	0.07	97.07
		55.19	0.19	22.42	2.33	0.03	0.16	2.83	6.90	8.90	0.05	0.70	0.27	0.03	95.88
		55.18	0.27	21.28	3.33	0.27	0.46	4.20	5.37	8.29	0.17	0.74	0.40	0.04	96.34
		56.79	0.34	21.06	3.39	0.02	0.21	2.29	6.02	8.78	0.04	0.76	0.15	0.15	96.03
		55.65	0.26	21.37	3.36	0.22	0.34	3.56	6.71	6.87	0.04	0.80	0.57	0.25	95.41
		56.26	0.36	20.48	3.84	0.19	0.48	4.18	6.06	6.96	0.00	0.73	0.23	0.22	94.05
		55.26	0.35	21.14	3.34	0.29	0.46	3.96	5.96	8.30	0.12	0.66	0.15	0.02	94.12

Supplementary Table S4: SEM-EDS single glass analyses of the Z-1 tephra for GC09 sediment core. All analyses recalculated water-free to 100%. The original totals are reported.

(Tephra) **t2**	(Sample) **PC12/VIII-96**	**SiO_2**	**TiO_2**	**Al_2O_3**	**FeO**	**MnO**	**MgO**	**CaO**	**Na2O**	**V_2O_3**	**Cr_2O_3**	**Original Total**
		37.52	0	0.16	24.77	0.5	35.29	0.44	0.07	0	0.06	98.81
		45.13	0	32.93	0.66	0	0.09	16.47	1.72	0.11	0	97.11
		50.82	1.16	1.99	8.83	0.14	13.19	21.21	0.5	0.12	0	97.96
		50.26	1.12	2.59	8.34	0.15	14.65	20.18	0.5	0.1	0	97.89
		49.09	1.3	3.63	8.68	0.24	13.34	20.96	0.64	0	0	97.88
		50.04	1.09	2.84	8.14	0.31	14.03	21.28	0.59	0.16	0	98.48
		37.42	0.04	0.15	22.33	0.56	37.76	0.27	0.14	0	0.04	98.71
		48.44	1.43	4.01	9.27	0.24	12.49	21.26	0.48	0.34	0	97.96
		47.33	1.54	5.11	8.1	0.02	13.21	21.73	0.53	0	0	97.57
		34.75	0.04	0.23	36.35	1.03	24.73	0.45	0.15	0	0	97.73
		37.41	0.26	0.15	22.27	0.41	37.21	0.28	0.19	0	0	98.18
		48.44	2.29	3.75	9.56	0.36	12.89	20.37	0.61	0.12	0	98.39
		36.49	0	0.17	25.86	0.51	33.61	0.22	0.12	0	0.25	97.23
		51	0	29.88	0.64	0.11	0.17	12.85	3.69	0	0.07	98.41
		47.92	1.81	4.69	9.12	0.45	13.09	20.65	0.56	0.18	0	98.47
		100.4	0.04	0.15	0.21	0	0.04	0.02	0	0.08	0.09	101.03

Supplementary Table S5. SEM-EDS analyses of clinopyroxene from cryptotephra t2 for PC12 sediment core.

(Tephra) **t3 (E-1)**	(Sample) **PC12/VI-261**	**SiO_2**	**TiO_2**	**Al_2O_3**	**FeO**	**MnO**	**MgO**	**CaO**	**Na_2O**	**K_2O**	**P_2O_5**	**Cl**	**F**	**S**	**Original Total**
		74.99	0.10	13.18	1.43	0.00	0.13	0.74	3.93	4.96	0.05	0.39	0.10	0.00	93.38
		74.68	0.10	13.31	1.49	0.00	0.14	0.86	4.05	4.97	0.00	0.40	0.00	0.00	94.21
		75.26	0.09	13.06	1.43	0.13	0.10	0.75	3.82	5.02	0.04	0.30	0.00	0.00	93.51
		75.10	0.00	13.14	1.39	0.05	0.08	0.75	3.85	4.95	0.06	0.38	0.00	0.24	93.24
		75.33	0.00	13.36	1.42	0.15	0.03	0.75	3.53	4.99	0.00	0.34	0.00	0.10	93.93
		74.64	0.09	13.31	1.60	0.17	0.02	0.87	3.82	4.94	0.00	0.33	0.25	0.00	93.56
		75.07	0.11	13.20	1.49	0.09	0.03	0.70	3.78	5.04	0.05	0.37	0.07	0.00	93.46
		74.80	0.01	13.15	1.73	0.17	0.10	0.80	3.80	5.07	0.10	0.29	0.00	0.00	93.52
		75.45	0.00	13.17	1.30	0.07	0.11	0.76	3.46	5.09	0.00	0.30	0.23	0.05	93.93
		75.21	0.03	13.32	1.57	0.09	0.05	0.63	3.68	5.06	0.00	0.38	0.00	0.00	92.73
		74.87	0.00	13.18	1.70	0.01	0.11	0.72	3.81	5.13	0.03	0.34	0.00	0.11	93.16
		75.27	0.00	13.10	1.49	0.00	0.03	0.75	3.98	4.95	0.04	0.37	0.04	0.00	93.53
		75.24	0.00	13.01	1.53	0.00	0.03	0.82	3.86	5.19	0.00	0.30	0.03	0.00	93.24
		74.78	0.00	13.18	1.45	0.00	0.13	0.78	4.05	5.03	0.13	0.32	0.04	0.09	93.17
		74.97	0.14	13.20	1.42	0.06	0.13	0.69	3.92	4.93	0.02	0.34	0.00	0.18	93.55

Supplementary Table S6: SEM-EDS single glass analyses of the E-1 tephra for PC12 sediment core. All analyses recalculated water-free to 100%. The original totals are reported.

(Tephra) **t4 (Y-1)**	(Sample) **PC12/III-563**	**SiO_2**	**TiO_2**	**Al_2O_3**	**FeO**	**MnO**	**MgO**	**CaO**	**Na_2O**	**K_2O**	**P_2O_5**	**Cl**	**F**	**S**	**Original Total**
		61.22	1.32	16.86	5.58	0.18	1.65	3.61	5.63	3.36	0.27	0.34	0.00	0.00	98.94
		61.01	1.45	16.34	6.39	0.21	1.82	3.30	5.74	3.23	0.21	0.30	0.00	0.00	99.29
		61.61	1.43	16.63	5.13	0.27	1.70	3.38	5.69	3.26	0.31	0.30	0.12	0.19	99.52
		62.24	1.33	16.23	5.31	0.20	1.54	2.82	5.56	3.78	0.41	0.42	0.03	0.13	98.7
		62.50	1.42	16.23	4.86	0.41	1.39	2.99	5.50	3.73	0.55	0.43	0.00	0.00	97.79
		62.87	1.38	15.85	4.76	0.32	1.36	2.96	5.59	3.80	0.56	0.47	0.00	0.06	95.85
		61.58	1.49	16.58	4.73	0.26	1.63	3.43	5.24	3.95	0.55	0.39	0.06	0.12	98.41
		62.68	1.34	16.12	4.97	0.22	1.47	3.12	5.37	3.47	0.46	0.44	0.19	0.17	98.22
		60.99	1.42	16.24	5.77	0.12	1.84	3.81	5.95	2.96	0.51	0.38	0.00	0.00	98.41
		62.38	1.29	16.45	4.99	0.07	1.65	3.43	5.55	3.43	0.45	0.32	0.00	0.00	98.82
		62.36	1.27	16.76	5.10	0.16	1.43	2.81	5.11	4.04	0.44	0.33	0.12	0.04	97.05
		63.14	1.37	16.82	4.06	0.25	1.41	2.77	5.64	3.86	0.40	0.21	0.06	0.00	97.76
		62.21	1.41	16.39	4.62	0.18	1.38	3.56	5.67	3.56	0.40	0.32	0.23	0.09	98.05
		61.28	1.44	16.80	5.04	0.25	1.69	3.71	5.17	3.89	0.34	0.35	0.05	0.00	98.16
		61.54	1.52	16.45	5.40	0.25	1.69	3.82	5.32	3.33	0.33	0.35	0.00	0.02	98.04

Supplementary Table S7: SEM-EDS single glass analyses of the tephra Y-1 for PC12 sediment core. All analyses recalculated water-free to 100%. The original totals are reported.

Tephra	**t1**												**t3**		**t4**	
Sample	**PC12/IX-47.5**				**PC12/IX-49**				**GC09/III-133.5**				**PC12/VI-261**		**PC12/III-563**	
n	4	σ	7	σ	12	σ	8	σ	8	σ	20	σ	15	σ		
SiO_2	55.31	*0.036*	54.85	*0.32*	55.41	*0.55*	54.97	0.26	55.29	*0.60*	55.25	*1.11*	75.04	*0.24*	61.97	*0.70*
TiO_2	0.19	*0.074*	0.45	*0.10*	0.21	*0.07*	0.50	0.05	0.29	*0.21*	0.42	*0.13*	0.04	*0.05*	1.39	*0.07*
Al_2O_3	22.86	*0.114*	21.09	*0.18*	22.61	*0.42*	20.93	0.14	22.45	*0.72*	20.85	*0.45*	13.19	*0.10*	16.45	*0.29*
FeO	2.25	*0.211*	3.44	*0.19*	2.34	*0.18*	3.70	0.18	2.48	*0.46*	3.81	*0.84*	1.50	*0.11*	5.11	*0.54*
MnO	0.12	*0.052*	0.12	*0.11*	0.13	*0.06*	0.11	0.07	0.10	*0.07*	0.16	*0.08*	0.07	*0.06*	0.23	*0.08*
MgO	0.17	*0.041*	0.48	*0.07*	0.15	*0.04*	0.47	0.08	0.14	*0.06*	0.55	*0.39*	0.08	*0.04*	1.58	*0.16*
CaO	2.81	*0.245*	4.24	*0.40*	3.10	*0.47*	4.35	0.28	2.76	*0.44*	4.11	*0.90*	0.76	*0.06*	3.30	*0.37*
Na2O	7.74	*0.179*	5.87	*0.28*	7.79	*0.94*	6.10	0.38	6.67	*1.06*	5.84	*0.95*	3.82	*0.16*	5.52	*0.23*
K_2O	7.32	*0.731*	8.08	*0.85*	6.84	*1.23*	7.50	0.52	8.61	*1.22*	7.82	*0.97*	5.02	*0.07*	3.58	*0.32*
P_2O_5	0.03	*0.038*	0.10	*0.03*	0.04	*0.05*	0.10	0.08	0.09	*0.06*	0.13	*0.09*	0.04	*0.04*	0.41	*0.11*
Cl	0.74	*0.067*	0.71	*0.05*	0.79	*0.10*	0.75	0.05	0.72	*0.07*	0.73	*0.08*	0.34	*0.04*	0.36	*0.07*
F	0.44	*0.143*	0.42	*0.12*	0.55	*0.16*	0.38	0.16	0.33	*0.14*	0.23	*0.12*	0.05	*0.08*	0.06	*0.08*
S	0.04	*0.008*	0.14	*0.05*	0.05	*0.06*	0.12	0.04	0.08	*0.08*	0.11	*0.09*	0.05	*0.07*	0.06	*0.07*
Original Total	98.83	*0.412*	98.43	*0.86*	97.60	*1.86*	98.36	0.59	97.18	*0.70*	96.35	*1.05*	93.47	*0.35*	98.20	*0.90*

Supplementary Table S8: Average composition of glasses representative of the studied tephras and cryptotephras. All analyses recalculated water-free to 100%. The original totals are reported, n: number of analyses; σ: standard deviation.

Planktonic foraminifera

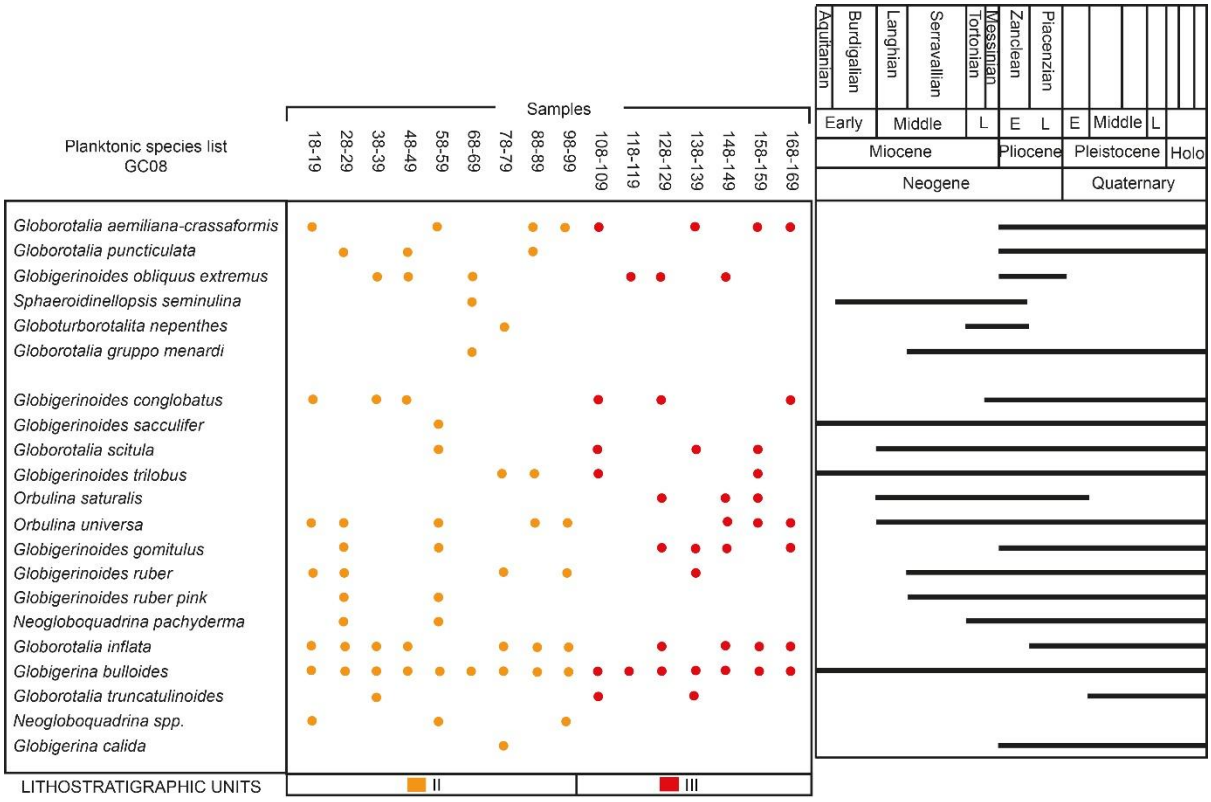

Supplementary Figure S1: The planktonic foraminiferal assemblages throughout the core span a wide stratigraphic range and consist of a mixture of late Miocene to late Quaternary species in various samples. Unit III and II in core PI23-GC08 contain marker species from the Mediterranean Miocene (*Globorotalia menardii* gr) and Pliocene (*Globorotalia margaritae*. *Globorotalia puncticulata*. *Globorotalia bononiensis*) time intervals.

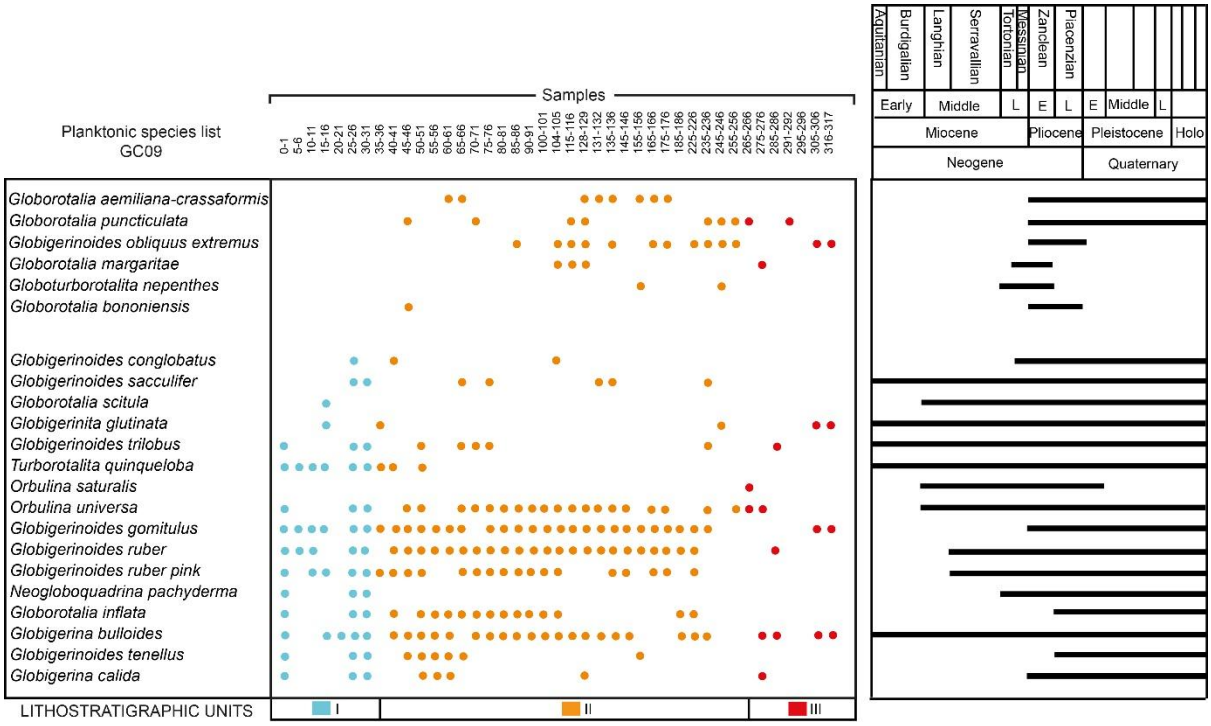

Supplementary Figure S2: The planktonic foraminiferal assemblages throughout the core span a wide stratigraphic range and consist of a mixture of late Miocene to late Quaternary species in various samples. Unit III and II in core PI23-GC09 contain marker species from the Mediterranean Miocene (*Globorotalia menardii* gr) and Pliocene (*Globorotalia margaritae*, *Globorotalia puncticulata*, *Globorotalia bononiensis*) time intervals. The uppermost part of core PI23-GC09 is characterized by the increase of taxa most abundant during the Late Quaternary (*i.e*. *Globigerinoides ruber pink*, *Globigerinoides trilobus*, *Globigerina bulloides*, *Neogloboquadrina pachyderma*).

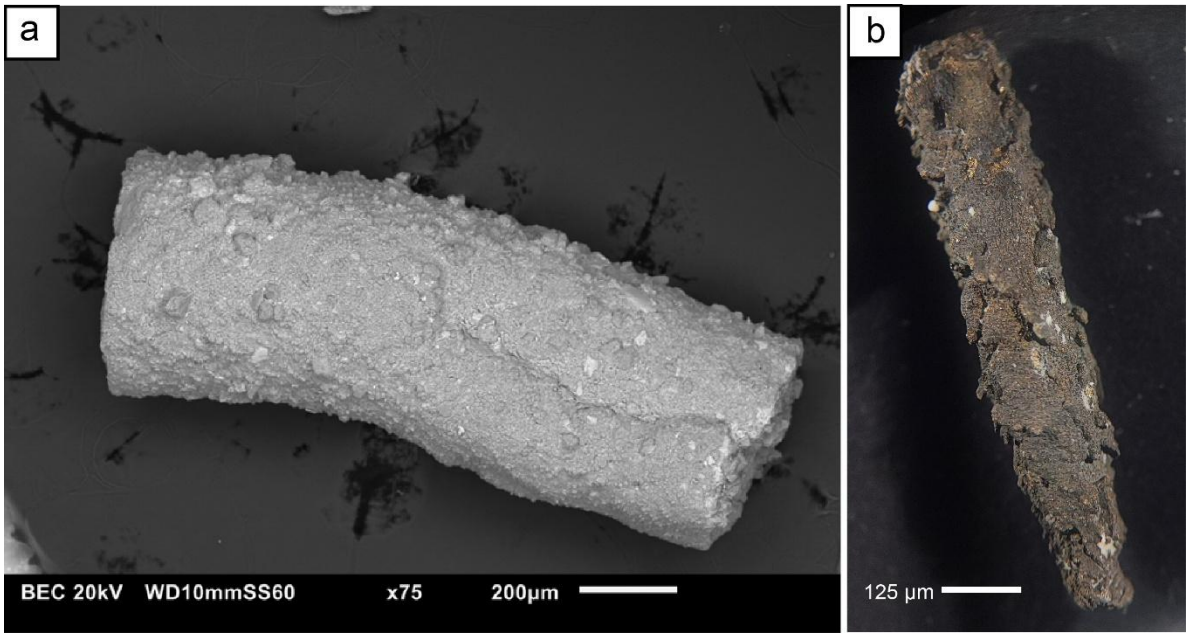

Supplementary Figure S3: Representative pyritized burrows from the GC09 sediment core (southern sector of the CMV). (a) Backscattered electron (BSE) SEM image of a specimen recovered from Unit III at 3.1 m bsf, showing an externally pyritized surface and a calcite-filling interior. Length of ~ 1.3 cm. (b) Photograph of a specimen recovered from Unit II at 1.8 m bsf, showing an externally pyritized surface. Length of ~ 1 cm.

REFERENCES

1. Sigurdsson, H. & Carey, S. The eruption of Vesuvius in AD 79. *Natl. Geogr. Res.* **1,** 332-387 (1985).
2. Keller, J., Ryan, W. B., Ninkovich, D. & Altherr, R. Explosive volcanic activity in the Mediterranean over the past 200,000 yr as recorded in deep-sea sediments. *Geol. Soc. Am. Bull.* **89,** 591-604 (1978).
3. Insinga, D. D. et al. The late Holocene tephra record of the central Mediterranean Sea: Mapping occurrences and new potential isochrons for the 4.4-2.0 ka time interval. *J. Quat. Sci.* **35,** 213-223 (2020).
4. Doronzo, D. M. et al. The 79 CE eruption of Vesuvius: A lesson from the past and the need of a multidisciplinary approach for developments in volcanology. *Earth-Sci. Rev.* **231,** 104072 (2022).
5. Polonia, A. et al. Large earthquakes along slow converging plate margins: Calabrian Arc paleoseismicity based on the submarine turbidite record. *Geosci. Front.* **14,** 101612 (2023).
6. Pepe, F. et al. Seismic stratigraphy of upper Quaternary shallow-water contourite drifts in the Gulf of Taranto (Ionian Sea, southern Italy). *Mar. Geol.* **397,** 79-92 (2018).
7. Crocitti, M. et al. On ash dispersal from moderately explosive volcanic eruptions: Examples from Holocene and Late Pleistocene eruptions of Italian volcanoes. *J. Volcanol. Geotherm. Res.* **385,** 198-221 (2019).
8. Di Donato, V. et al. The palaeoclimatic and palaeoceanographic history of the Gulf of Taranto (Mediterranean Sea) in the last 15 ky. *Glob. Planet. Change* **172,** 278-297 (2019).
9. Lippert, A. et al. Holocene onshore/offshore tephra correlation of Mt. Etna, Sicily. *Bull. Volcanol.* **87,** 4 (2024).
10. Coltelli, M., Del Carlo, P. & Vezzoli, L. Stratigraphic constraints for explosive activity in the past 100 ka at Etna Volcano, Italy. *Int. J. Earth Sci.* **89,** 665-677 (2000).
11. Sulpizio, R., Van Welden, A., Caron, B. & Zanchetta, G. The Holocene tephrostratigraphic record of Lake Shkodra (Albania and Montenegro). *J. Quat. Sci.* **25,** 633-650 (2010).
12. Albert, P. G. et al. Glass geochemistry of pyroclastic deposits from the Aeolian Islands in the last 50 ka: A proximal database for tephrochronology. *J. Volcanol. Geotherm. Res.* **336,** 81-107 (2017).
13. Paterne, M., Guichard, F. & Labeyrie, J. Explosive activity of the South Italian volcanoes during the past 80,000 years as determined by marine tephrochronology. *J. Volcanol. Geotherm. Res.* **34,** 153-172 (1988).
14. Siani, G., Sulpizio, R., Paterne, M. & Sbrana, A. Tephrostratigraphy study for the last 18,000 14C years in a deep-sea sediment sequence for the South Adriatic. *Quat. Sci. Rev.* **23,** 2485-2500 (2004).
15. Cosentino, C. et al. Benthic foraminifera as indicators of relative sea-level fluctuations: Paleoenvironmental and paleoclimatic reconstruction of a Holocene marine succession (Calabria, south-eastern Tyrrhenian Sea). *Quat. Int.* **439,** 79-101 (2017).

16. Di Roberto, A. et al. Tephrochronology of the NDT09 core in the Marsili Basin: Implications for the timing and dynamics of volcanic eruptions of the southern Tyrrhenian in the last c. 15 ka. *Bull. Volcanol.* **87,** 124 (2025).
17. Albert, P. G. et al. Late glacial explosive activity on Mount Etna: Implications for proximal-distal tephra correlations and the synchronisation of Mediterranean archives. *J. Volcanol. Geotherm. Res.* **265,** 9-26 (2013).
18. Siani, G. et al. Mediterranean Sea surface radiocarbon reservoir age changes since the Last Glacial Maximum. *Science* **294,** 1917-1920 (2001).
19. Lourens, L. J. Revised tuning of Ocean Drilling Program Site 964 and KC01B (Mediterranean) and implications for the δ18O, tephra, calcareous nannofossil, and geomagnetic reversal chronologies of the past 1.1 Myr. *Paleoceanography* **19,** PA3010 (2004).
20. Insinga, D. D. et al. Tephrochronology of the astronomically-tuned KC01B deep-sea core, Ionian Sea: Insights into the explosive activity of the central Mediterranean area during the last 200 ka. *Quat. Sci. Rev.* **85,** 63-84 (2014).